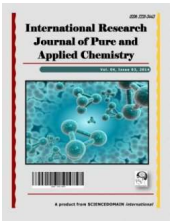

International Research Journal of Pure & Applied Chemistry
13(4): 1-14, 2016; Article no.IRJPAC.31542
ISSN: 2231-3443, NLM ID: 101647669

SCIENCEDOMAIN *international*
www.sciencedomain.org

Effect of Mono and Multivalent Dopants on Electrical Conductivity and Solid-State ^{1}H NMR Spectra of Polyaniline

Akira Kawahara[1], Shigeyuki Tsuji[2] and Hisashi Honda[1,2,3*]

[1]International Graduate School of Arts and Sciences, Yokohama City University, Yokohama 236-0027, Japan.
[2]Faculty of Science, Yokohama City University, Yokohama 236-0027, Japan.
[3]Graduate School of Nanobioscience, Yokohama City University, Yokohama 236-0027, Japan.

Authors' contributions

This work was carried out in collaboration between all authors. Author HH designed the study, performed the analysis and wrote the first draft of the manuscript. Authors AK and ST performed preparation and measurements of the samples and analyzed the results obtained in the study. All authors read and approved the final manuscript.

Article Information

DOI: 10.9734/IRJPAC/2016/31542
Editor(s):
(1) Martin Kroger, Department of Materials, Computational Polymer Physics, Swiss Federal Institute of Technology (ETH Zürich), Switzerland.
Reviewers:
(1) Fahmida Khan, National Institute of Technology, Raipur, India.
(2) Shunjin Peng, Wuhan University of Science and Technology, P.R. China.
Complete Peer review History: http://www.sciencedomain.org/review-history/17793

Original Research Article

Received 12th January 2017
Accepted 3rd February 2017
Published 10th February 2017

ABSTRACT

Solid-state ^{1}H nuclear-magnetic-resonance (NMR) measurements of polyaniline doped by $HClO_4$, H_2SO_4, and H_3PO_4 were performed with magic-angle-spinning (MAS) methods to reveal the effects of protonation on chain arrangements and the electrical conductivity of polyaniline. In this study, scanning electron microscopy (SEM) and X-ray diffraction (XRD) measurements were also carried out. Electrical conductivity measurements showed that polyaniline doped by $HClO_4$ had a large conductivity as compared with polyaniline prepared with H_2SO_4 and H_3PO_4 dopants. In addition, ^{1}H MAS NMR spectra revealed that the ratio of $-NH^+=$ and $-NH_2^+-$ sites increased with increasing dopant concentration in the polymers. The linewidths of the ^{1}H MAS NMR signals of polyaniline doped by $HClO_4$ were similar to those polymerized from aniline-*d*5 ($C_6D_5NH_2$) in $HClO_4$ solution.

**Corresponding author: E-mail: hhonda@yokohama-cu.ac.jp;*

Based on this result, polyaniline can undergo fast motions in the solids. NMR, SEM and XRD spectra suggest that multivalent dopants of H_2SO_4 and H_3PO_4 construct polymer blocks in the solids and that the blocks contribute to their low electrical conductivities.

Keywords: ^{1}H MAS NMR; polyaniline; electrical conductivity; SEM; XRD.

1. INTRODUCTION

Conducting polymers have been widely investigated in the chemical industry with scientific endeavors carried out since the discovery of polyacetylene [1]. Polyaniline (PAN), a conducting polymer, has achieved significant importance among conducting polymers because it possesses good environmental stability [2,3] and is easily prepared by chemical or electrochemical oxidation of aniline in acidic solution [4-9]. The 'doped' (protonated) form of PAN (abbreviated to DopedPAN) becomes green and has high conductivity at the semiconductor level on the order of 10^{-2} - 10^{3} S cm^{-1}. The most probable configuration of DopedPAN is the emeraldine-salt form (Fig. 1), which is obtained by an oxidative polymerization of aniline in acidic

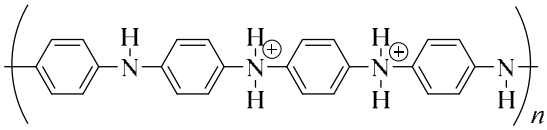

Leuco Salt (Reduction Type) Insulator, Clear Color

Reduction ↑↓ Oxidation

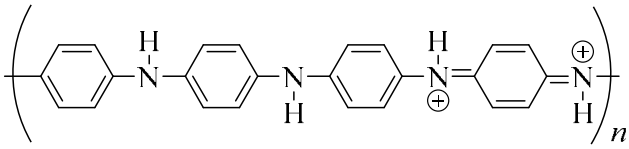

Emeraldine Salt (Acid Condition) (Oxidation Type I) Conductor, Green Color

H^+ ↑↓ $-H^+$

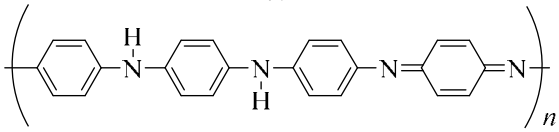

Emeraldine Base (Base Condition) (Oxidation Type I) Insulator, Dark Blue Color

Oxidation ↑↓ Reduction

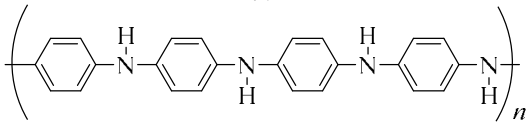

Leucoemeraldine (Reduction Type) Insulator, Yellow Color

Reduction ↑↓ Oxidation

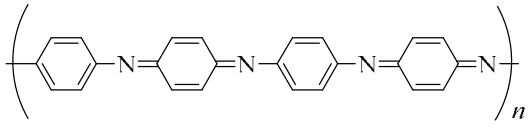

Pernigraniline (Oxidation Type II) Insulator, Black or Dark Purple Color

Fig. 1. Reported chemical formula of polyaniline [7-10] for the (a) Leuco salt, (b) emeraldine salt, (c) emeraldine base, (d) leucoemeraldine, and (e) pernigraniline. The emeraldine salt shows electrical conductivity

solutions [7-10]. Employing acids, e.g., perchlorate acid, sulfonic acid, phosphoric acid, etc., cation radicals (polarons) are doped on the nitrogen atoms of PAN by the acids. The positive charge on the PAN chains is neutralized by the counter anions of the doped acid (ClO_4^-, SO_4^{2-}, PO_4^{3-}, etc.). The conductivity path is proposed to be a quasi-one dimensional diffusion of electrons on the polymer. Moreover, conductivity depends on molecular linkages among polymer chains and dopants, i.e., the polymer chain conformation (interpolymer packing) and the charge distribution on the polymer chain [11-14].

Solid-state nuclear-magnetic-resonance (NMR) is a powerful tool to reveal molecular interactions between polymers and dopants and to obtain information about the chemical environment of the polymer. Some previously reported ^{13}C and ^{15}N NMR spectra of DopedPAN and DedopedPAN (the deprotonated polymer) revealed the polymer chain conformations of each [15-24]. These studies suggested that the conformation of PAN is dependent on the preparation conditions. The ^{13}C NMR spectra showed broad linewidths, although magic-angle-spinning (MAS) and cross-polarized (CP) methods were applied. The origin of broad signals could be explained by the dispersion of chemical shift (CS) over the polymers since various polymer conformations are mixed in the solids and electron delocalization is partially disrupted on the polymer. In conductive materials, a Knight shift is frequently detected in ^{13}C NMR spectra; however, DopedPANs showed slight CS shifts relative to the dedoped states [18,19,25-30]. In the case of ^{15}N nuclei, NMR spectra revealed alternating benzenoid and quinoid repeating units in the emeraldine salts [20,31-34], as displayed in Fig. 1. Unpaired electrons were also reported in the ordered crystalline regions of DopedPAN [22]. Rotational-echo and double-resonance (REDOR) experiments in a copolymer of PAN revealed that the amorphous regions of PAN chains were arranged with an in-plane inter-chain separation of ca. 1 nm [22]. Furthermore, ^1H NMR spectra of DopedPAN dissolved in aqueous solution showed the relationship with protonation and conductivity with a larger concentration of dopants resulting in higher conductivity [35]. As described above, NMR is a powerful tool to reveal chain arrangements and the chemical environments of solid state PAN. However, high-resolution solid-state ^1H MAS NMR spectra of DopedPAN are rarely reported, although protonation effects on chain arrangements is linked to the conductivity of solid PAN. Since ^1H MAS NMR lines are sensitive to small changes in molecular interaction and motion [36-45], ^1H MAS NMR spectra measurements were performed to reveal the effects of protonation on chain arrangements and conductivity in DopedPAN.

2. EXPERIMENTAL

In order to prepare PAN samples in acidic solution, the following processes were performed separately. First, 3.0 g of aniline (Wako) was added to 60.0 g of distilled water. Then, 5.0, 8.2, and 12.6 g of H_2SO_4 (95%, Wako) was poured into the solution, which corresponds to 8, 13, and 20 wt% of the aniline solution, respectively. After dissolving the aniline salts completely in the solution, two Pt plates (1.5×3.0 cm) were placed in the solution, and direct current of 1.0 V was applied for 4 hours. From this electrochemical reaction, doped PAN was synthesized on the anode. To prepare dedoped PAN, another sample of doped PAN was placed on a Pt plate, and an inversion current was applied to both plates until the current flow decreased. The doped and dedoped-PAN were shaved off from each plate, washed with water, and dried under air for two days. In this study, we use the symbols DopedPAN (*x* H_2SO_4) and DedopedPAN (*x* H_2SO_4) for doped and dedoped PAN, respectively, where *x* is the concentration of H_2SO_4 in wt%. A similar preparation was used with $HClO_4$ (Kantou Kagaku) or H_3PO_4 (Kantou Kagaku), and we obtained DopedPAN (*x* $HClO_4$), DedopedPAN (*x* $HClO_4$), DopedPAN (*x* H_3PO_4), and DedopedPAN (*x* H_3PO_4) individually. In order to discuss ^1H NMR spectra, a deuterium substituted sample of DopedPAN (13 $HClO_4$) was prepared using aniline-*d*5 (98%, Kantou Kagaku), in which the five H atoms in the benzene ring are substituted with D atoms ($C_6D_5NH_2$). This polymer is called DopedPAN (13 $HClO_4$)-*d* in this study.

Solid-state ^1H NMR spectra were recorded at a Larmor frequency of 600.13 MHz using a Bruker Avance 600 spectrometer (14.09 T). The polymers were packed in a ZrO_2 rotor with an outer diameter of 2.5 mm. The spectra were observed using the MAS method with a MAS speed of 10, 20, and 30 kHz. The signals were recorded by a Fourier transformation of the free-induction-decay (FID) signals obtained after a π/2 pulse. The ^1H NMR chemical shifts (CSs) were calibrated relative to a silicon rubber internal standard (δ = 0.12 ppm). The spin lattice

relaxation time (T_1) was estimated using an inversion recovery method (π_x - t - $(\pi/2)_x$ - FID), and the recycle time was set to 30 s.

In order to confirm the crystal structure of the prepared specimens, powder X-ray diffraction (XRD) patterns were measured by a Rigaku RAD-X in a scan range of 5 - 40° in steps of 0.02° with a Cu anticathode. Electrical-conductivity measurements were performed with an Advantest R6144 DC power supply and a Keithley 2000 Multimeter. To measure the conductivity, the polymer sample was pressed into a 1 cm diameter disc at 20 atm and set between two Cu plates. Scanning electron microscope (SEM) photographs were obtained using a Keyence VE-9800 at a pressure of 6.7×10^{-2} Pa.

3. RESULTS AND DISCUSSION

3.1 Electrical Conductivity

Resistance values for each sample were estimated by the slope of the voltage-current plot as displayed in Fig. 2. In the case of DopedPAN (x $HClO_4$), the voltages were proportional to the current in a wide range so that Ohm's law could be established. In contrast, the slopes of DopedPAN (13 H_2SO_4) and DopedPAN (8 H_3PO_4) drastically increased with the current at around 0 A. Therefore, slopes obtained at around -0.03 μA were employed for estimating the resistances in DopedPAN (x H_2SO_4) and DopedPAN (x H_3PO_4). Electrical conductivities were estimated by measuring the thickness of disc with the electrical conductivity obtained at

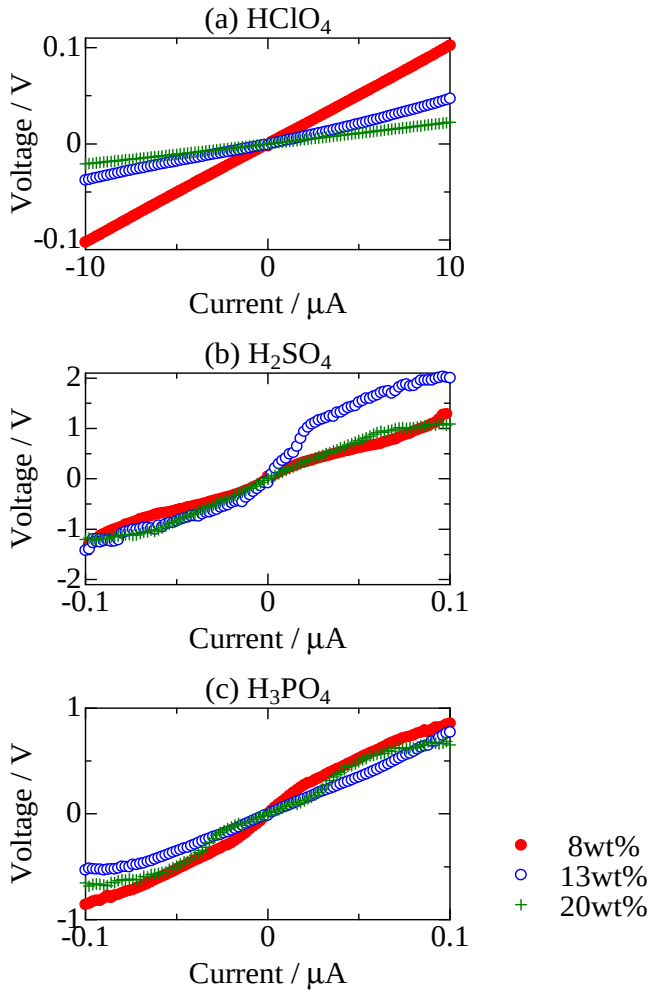

Fig. 2. Voltage-current plot of doped polyaniline (solid) prepared in (a) $HClO_4$, (b) H_2SO_4, and (c) H_3PO_4 solution. Here, the red solid circle, blue open circle, and green cross denote dopant concentrations of 8, 13, and 20 wt% in each solution, respectively

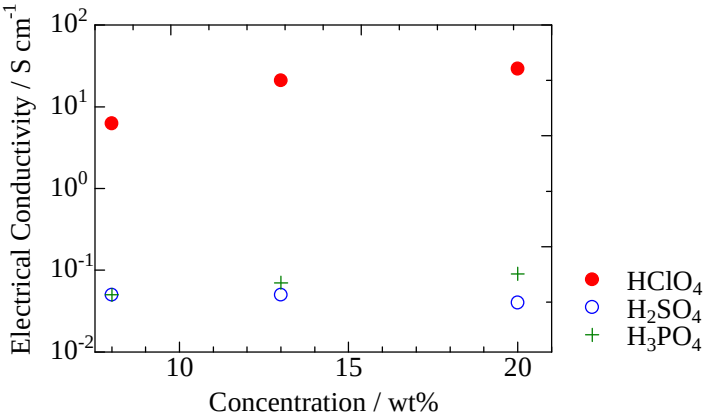

Fig. 3. Electrical conductivity of solid polyaniline as a function of dopant concentration. Here, the red solid circle, blue open circle, and green cross correspond to $HClO_4$, H_2SO_4, and H_3PO_4, respectively

298 K shown in above Fig. 3. These results show that the electrical conductivity of DopedPAN (*x* $HClO_4$) was correlated to the concentration of *x* and was much greater than those of DopedPAN (*x* H_2SO_4) and DopedPAN (*x* H_3PO_4). In order to reveal the different characters of these samples, ^{1}H MAS NMR measurements were carried out.

3.2 NMR

The ^{1}H MAS NMR spectra observed in DopedPAN (13 $HClO_4$) and DedopedPAN (13 $HClO_4$) with a MAS rate of 30 kHz are shown in Figs. 4a and 4b, respectively. The spectra can be roughly separated by two peaks: one detected at ca. 2 ppm and another at ca. 7 ppm. In these figures, the results of line analyses are also displayed. The signals recorded at ca. 2 and 7 ppm can be immediately assigned to H atoms bonded to N atoms and benzene rings in PAN, respectively. In addition, the ^{1}H MAS NMR spectra show similar linewidths in DopedPAN and DedopedPAN. This result suggests that paramagnetic effects on ^{1}H NMR spectra are small. In order to estimate dipole-dipole interaction among H atoms in the solid, a ^{1}H MAS NMR spectrum was also measured in the deuterated polymer sample DopedPAN (13 $HClO_4$)-*d* described above. The ^{1}H MAS NMR envelopes recorded for DopedPAN(13 $HClO_4$)-*d* with MAS = 30 kHz are shown in Fig. 4c. The signal intensity of -NH- (2 ppm) was larger than that of the benzene ring (7 ppm) caused by the 2% ^{1}H in aniline-*d*5 used to prepare the polymer. This fact guarantees our assignment of the peaks described above. In ^{1}H NMR spectra, linewidths are generally determined by dipole-dipole interaction among H atoms. The Hamiltonian of the dipole-dipole interaction ($\mathcal{H}_{\mathrm{d}}$) between homo- and hetero-nuclei is shown as follows [46,47]:

$$\mathcal{H}_{\mathrm{d}}^{\mathrm{homo}} = \gamma^2\hbar^2 \sum_i \sum_j \frac{\left(1-3\cos^2\theta_{ij}\right)}{r_{ij}^3}\left[\hat{I}_{iz}\hat{I}_{jz} - \frac{1}{4}\left(\hat{I}_i^+\hat{I}_j^- + \hat{I}_i^-\hat{I}_j^+\right)\right] \quad (1)$$

$$\mathcal{H}_{\mathrm{d}}^{\mathrm{hetero}} = \hbar^2 \sum_i \sum_j \frac{\gamma_i\gamma_j\hat{I}_{iz}\hat{I}_{jz}}{r_{ij}^3}\left(1 - 3\cos^2\theta_{ij}\right) \quad (2)$$

Here, *i* and *j* are number of the nuclei, γ is a gyromagnetic ratio, r_{ij} and θ_{ij} are the distance between *i* and *j* and the angle between the vectors of the static magnetic field and the $\boldsymbol{r}_{ij}$ vector, respectively, and $\hat{I}$ is the nuclear spin operator with the direction of static magnetic-field along the *z* axis. The average distances of ^{1}H-^{1}H in the natural abundance samples were much closer than those in the D enriched sample in which ^{1}H nuclei of ca. 2% were distributed over the benzene ring of DopedPAN (13 $HClO_4$)-*d* polymers. In addition, the γ value of D is smaller than that of H ($\gamma_D = 0.15\gamma_H$) [46]. Therefore, by substituting H atoms for D atoms, ^{1}H NMR spectra with reduced linewidths can be recorded in ordinal crystals, such as glycine-*d*5, as demonstrated in Fig. 5. As shown in Figs. 4a and 4c, similar linewidths were recorded at 7 ppm for DopedPAN(13 $HClO_4$)-*d* and DopedPAN (13 $HClO_4$), although dipole-dipole interaction among

H atoms of the benzene ring was reduced in the former. In the case of the glycine-*d*5 crystal, whole H atoms bonded to the N atom are located in the same chemical environment. Therefore, only one CS value can be recorded on a ^{1}H MAS NMR spectrum; in contrast, the two H atoms of -CH_2- in a glycine molecule are located in different environments in its crystal. Based on these results, the linewidths of the ^{1}H NMR spectra in DopedPAN could be caused by the distribution of polymers since various chemical environments of the benzene ring are mixed in the solid. This consideration is consistent with previous ^{13}C NMR spectra measurements [15-24]. In addition, our results indicate that benzene rings undergo fast motion (e.g., reorientation motion about the main chain) in the DopedPAN solid. In order to estimate the chain's motions in the polymer, the dependence of linewidth on MAS rate was measured as shown for DopedPAN (*x* $HClO_4$) in Fig. 6. This figure indicates that similar linewidths were recorded for each ^{1}H MAS NMR spectrum, although different MAS rates were applied. In general, linewidths of ^{1}H MAS NMR spectra are strongly dependent on the MAS speeds in ordinal crystals such as glycine since molecular motions are restricted in the crystal, as demonstrated in Fig. 7. The line-shapes shown in Fig. 6 also support that dipole-dipole interaction among the H atoms in the polymers is small. The linewidths estimated in the doped and dedoped samples are listed in Table 1. These results suggest that dipole-dipole averaging by the MAS method is slightly more effective in the doped polymer than the dedoped polymer because molecular motions in the doped sample are slightly slower.

Table 1. Linewidths of DopedPAN (13 $HClO_4$) and DedopedPAN (13 $HClO_4$) recorded at ca. 7 ppm as a function of MAS rates

MAS rate / kHz	Line width / ppm	
	DopedPAN	DedopedPAN
10	10.7	6.2
20	7.9	5.5
30	5.3	5.0

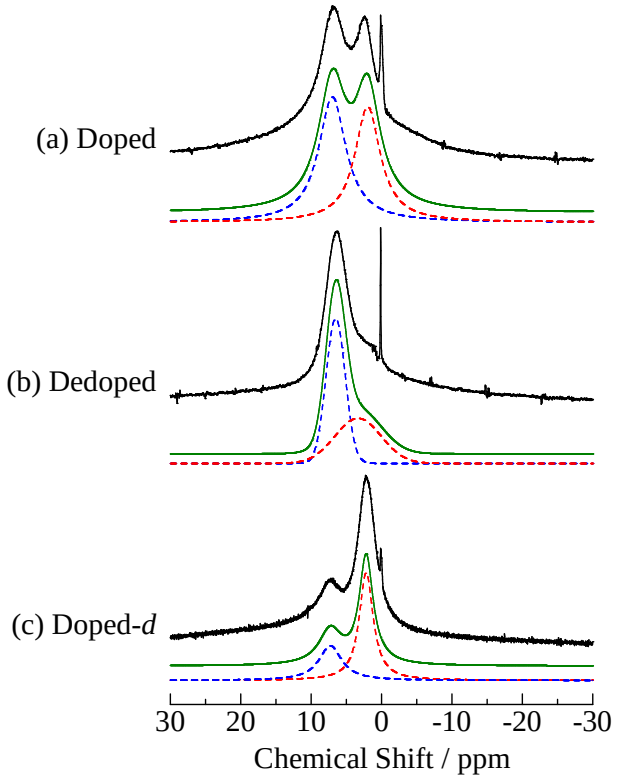

Fig. 4. Solid-state ^{1}H MAS NMR spectra observed in polyaniline (a) doped with 13 wt% $HClO_4$ aqua solution, (b) dedoped, and (c) polymerized using aniline-*d*5 ($C_6D_5NH_2$). These lines were recorded with a MAS rate of 30 kHz. Here, the signal recorded at 0.12 ppm is assigned to silicon rubber (reference) on each spectrum. The green lines are the envelope obtained by summing the Gaussian functions shown as red and blue dashed lines

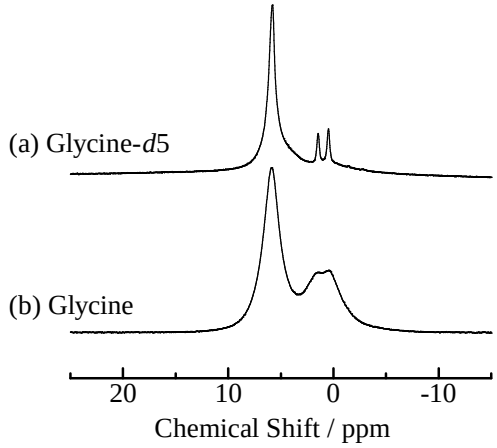

Fig. 5. Solid-state ^{1}H MAS NMR spectra observed in (a) glycine-*d*5 (ND_2CD_2COOD) and (b) glycine crystals. The NMR spectra were recorded with a MAS speed of 35 kHz. These line envelopes showed that dipole-dipole interaction among H atoms was drastically reduced by deuterium substitution in the glycine-*d*5 crystal since H atoms of ca. 2% are substituted in the crystal

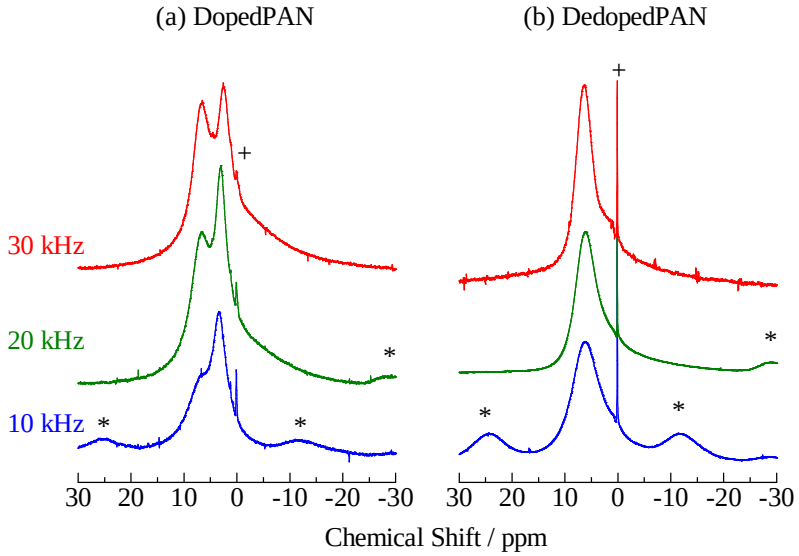

Fig. 6. MAS speed dependences of ^{1}H MAS NMR spectra observed in (a) polyaniline doped by 13 wt% $HClO_4$ and (b) its dedoped sample. The values of 10, 20, and 30 kHz are MAS speeds. The symbols of + and * denote the peak of an internal standard sample (silicon rubber) and the spinning sidebands with an observed frequency of 600.13 MHz, respectively

The signal intensity observed at ca. 2 ppm was reduced in the dedoped samples as shown in Figs. 4a and 4b. To compare the samples, the area under the signal recorded at 2 and 7 ppm was first estimated by a Gaussian function. Then, a relative area could be obtained by dividing the area at 2 ppm by that at 7 ppm. The relative area slightly decreased from a value of 0.85 for the doped polymer to 0.74 for the dedoped polymer. These results suggest that some of the -NH- groups formed $-NH_2^+-$ in the doped polymer and that $HClO_4$ was removed from the polymer and went back into solution by applying the inversion current (a reduction process) as illustrated in Fig. 8. In this model, the dedoped chemical formula is agreement with that reported in the reference [48].

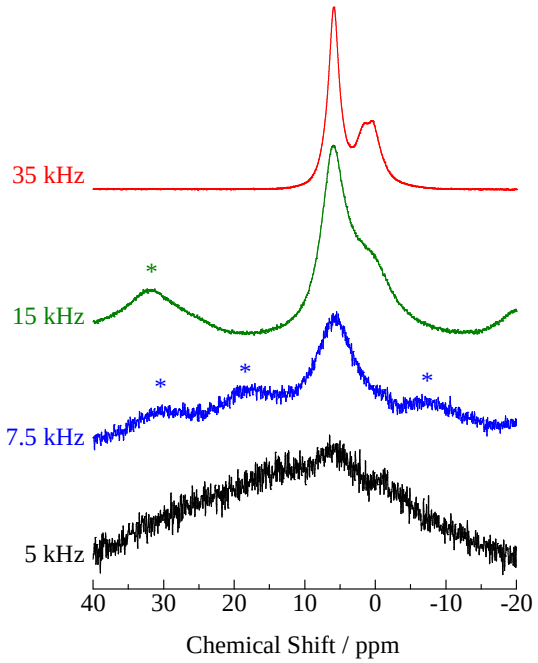

Fig. 7. MAS speed dependences of ^{1}H MAS NMR spectra observed in glycine crystals. The values of 5, 7.5, 15, and 35 kHz are MAS rates. In this figure, the symbol of * denotes the spinning sidebands with an observed frequency of 600.13 MHz

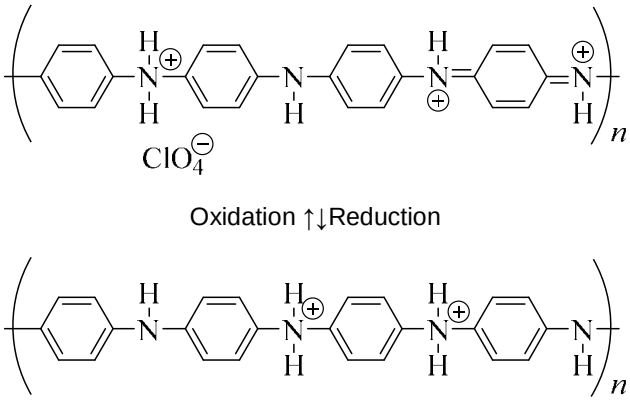

Fig. 8. A model that can explain the results of our ^{1}H MAS NMR measurements displayed in Figs. 4 and 9

In order to evaluate the effect of the dopant, ^{1}H MAS NMR spectra of DopedPAN (*x* $HClO_4$), DopedPAN (*x* H_2SO_4), and DopedPAN (*x* H_3PO_4) with a MAS rate of 30 kHz were observed as a function of dopant concentration *x*. In these polymers, signal intensities observed at ca. 2 ppm increased relative to those recorded at ca. 7 ppm with increasing *x* values as displayed in Fig. 9. This tendency also suggests that addition of H atoms to the N atoms increases successively with increased dopant concentration (Fig. 8). The linewidths of DopedPAN (*x* H_2SO_4) and DopedPAN (*x* H_3PO_4) were slightly broad as compared with those of DopedPAN (*x* $HClO_4$). Based on these results, chemical environments can be widely distributed over the polymers doped by double and triple valent acids as compared with monovalent acids ($HClO_4$).

In addition, each peak recorded at ca. 2 and 7 ppm shifted with increasing *x* values as shown in Fig. 10. The CS value of H atoms bonded to the

N atom increased in DopedPAN (*x* $HClO_4$) with increasing *x* values, whereas those of DopedPAN (*x* H_2SO_4) and DopedPAN (*x* H_3PO_4) decreased. In contrast, the values of H atoms bonded to benzene ring in the whole compounds slightly increased with increasing *x* values. In the case of H atoms in benzene rings, ring currents make an induced magnetic field at the H atoms parallel to the static field, which results in large ^1H CS values. Because CS values slightly increased with increasing concentration of dopant, a large current can be induced by increasing the dopant concentration in each sample. This tendency is consistent with the result of our conductivity measurements as shown in Fig. 3. Comparing CS values among the three dopants, the CS values of DopedPAN (*x* H_3PO_4) were smaller than those of the others, although three H atoms can be linked to the polymers with the same *x* values. In addition, small slopes were obtained for DopedPAN (*x* H_2SO_4) and DopedPAN (*x* H_3PO_4), compared with those of DopedPAN (*x* $HClO_4$). These results suggest that the multivalent acids prevent conductivity in their polymers. This consideration is consistent with the conductivity measurements as displayed in Fig. 3, in which the electric resistances of DopedPAN (*x* H_2SO_4) and DopedPAN (*x* H_3PO_4) were larger than those of DopedPAN (*x* $HClO_4$).

Before the origin of the lower conductivities recorded for the multivalent dopants is described, we discuss the dopant concentration dependence of the ^1H NMR CS values of H atoms linked to the N atom. As demonstrated in Fig. 10, the CS values increased in DopedPAN (*x* $HClO_4$); in contrast, the opposite tendency was detected in the multivalent dopants. The diamagnetic terms of the shielding tensors are well known to mainly affect the ^1H NMR CS values as compared with the paramagnetic terms, and the diamagnetic term increases with electron density [46,47]. Therefore, the lower electron density at an H atom corresponds to larger ^1H CS values. As shown in Fig. 8, three kinds of H atoms contribute to the signal recorded at 2 ppm in the doped material: -NH-, -NH^+=, and -NH_2^+-. These H atoms could not be distinguished from each other on the ^1H MAS NMR spectra (Figs. 4 and 9) since each signal from -NH-, -NH^+=, and -NH_2^+- was superimposed on the spectra. It can be assumed that electron density at H atoms of -NH^+= and -NH_2^+- is smaller than that of -NH- since the electron density of a positive atom is smaller than that of neutral atom. Therefore, the CS value increased with increasing $HClO_4$ concentration because the relative ratio of signal intensities corresponding to -NH^+= and -NH_2^+- increased while that of -NH- decreased, and whole dopants of $HClO_4$ were linked to the N atoms in the polymer. This model is consistent with our electrical conductivity measurements, in which conductivity increased with increasing $HClO_4$ concentration in the polymer. In contrast, the H_2SO_4 and H_3PO_4 dopants attracted some of the -NH_2^+- sites on the polymers and thus constructed rigid cores in the solid. Consequently, two paths for electrical conductivity in polyaniline are proposed: one on the polymer chain and one between the chains [11-14]. The electrical resistance of the latter path is generally larger than that of the former process. Therefore, electron transfers between the chains are prevented if many rigid cores are distributed over the solid since in general, contact resistance between the harder parts of conductors becomes larger because of small contact areas. In order to obtain structural information about the solid states of the polymers, SEM and XRD measurements were carried out.

3.3 SEM and XRD

SEM photographs for DopedPAN (*x* $HClO_4$), DopedPAN (*x* H_2SO_4), and DopedPAN (*x* H_3PO_4) are shown in Fig. 11. Based on these photographs, DopedPAN (*x* $HClO_4$) can be classified into stick-type solids; conversely, block-type structures were observed in the others. This difference is consistent with the models we proposed based on the results of NMR measurements. XRD spectra obtained for each polymer are displayed in Fig. 12. Similar XRD patterns were recorded in DopedPAN (*x* $HClO_4$) for each concentration. Conversely, the line patterns of DopedPAN (*x* H_2SO_4) and DopedPAN (*x* H_3PO_4) were dependent on *x*; the signal intensity observed at a low angle of ca. 15° decreased with decreasing dopant concentration. The peaks recorded on our XRD spectra correlate to the distance between polymers and/or the blocks constructed by dopants since the polymers assembled around each dopant. Because signals detected at the lower angles of the XRD spectra correspond to longer separations, ratios of the long-distance component decreased with increasing concentration of *x* in DopedPAN (*x* H_2SO_4) and DopedPAN (*x* H_3PO_4). Each polymer treated in this study was prepared in solution; therefore, it can be assumed that the dopants are homogeneously distributed over the samples.

Based on our results of electrical conductivity, SEM, XRD, and NMR measurements, we can illustrate a model that shows multivalent dopants forming polymer blocks.

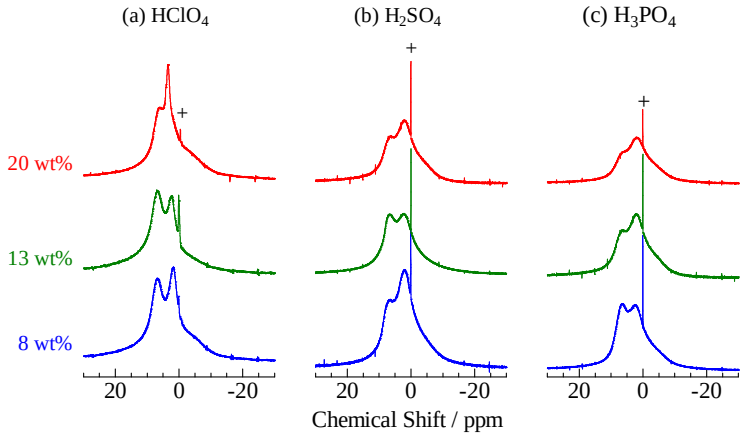

Fig. 9. Solid-state ^{1}H MAS NMR spectra observed in polyaniline doped with (a) $HClO_4$, (b) H_2SO_4, and (c) H_3PO_4. The values of 8, 13, and 20 wt% are the dopant concentrations. In this figure, + denotes the peak of silicon rubber (reference)

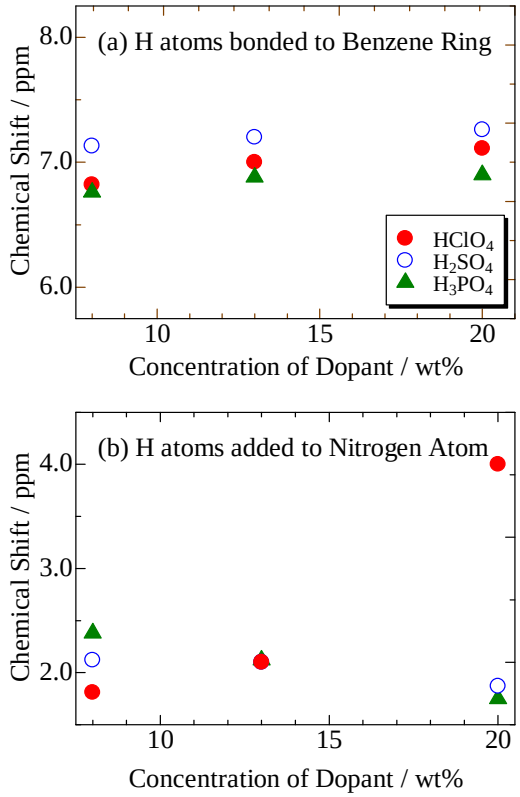

Fig. 10. Observed chemical shift as a function of dopant concentration. (a) The chemical shift of H atoms bonded to benzene ring in polyaniline. (b) The values of H atoms added to the N atoms in the polymer. Here, the red solid circle, blue open circle, and green cross correspond to $HClO_4$, H_2SO_4, and H_3PO_4, respectively. Similar values were obtained in each polyaniline prepared with a 13 wt% solution of each dopant

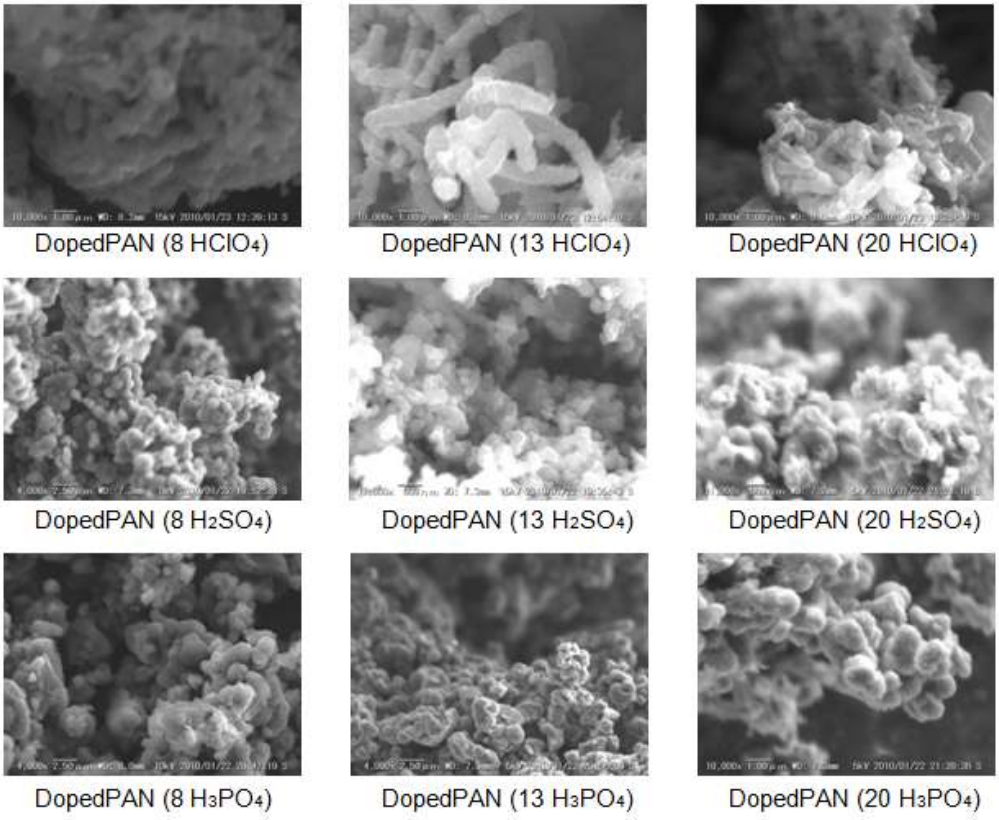

Fig. 11. SEM photographs of polyaniline doped by $HClO_4$, H_2SO_4, and H_3PO_4. The values of 8, 13, and 20 are the dopant concentrations in wt%. Block-type structures were observed in the polyaniline doped by H_2SO_4 and H_3PO_4

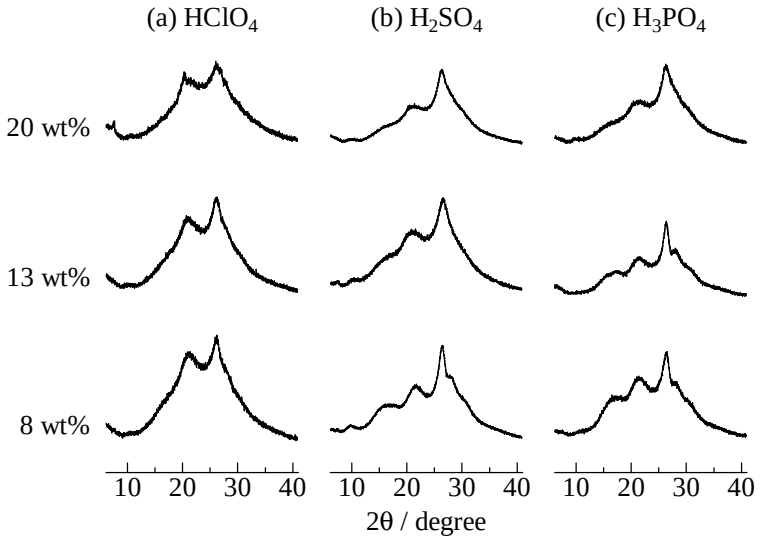

Fig. 12. XRD spectra of polyaniline doped by (a) $HClO_4$, (b) H_2SO_4, and (c) H_3PO_4. The values of 8, 13, and 20 are the dopant concentrations in wt%

4. CONCLUSION

We measured the electrical conductivity, ^{1}H MAS NMR spectra, SEM photographs, and XRD lines in polyanilines doped by $HClO_4$, H_2SO_4, and H_3PO_4 with various concentrations. The electrical conductivity of DopedPAN (*x* $HClO_4$) was larger than those of H_2SO_4 and H_3PO_4. Solid-state high-resolution ^{1}H MAS NMR measurements were performed to reveal the effects of protonation on chain arrangements. Based on our ^{1}H MAS NMR measurements, the -NH_2^+- and -NH^+= sites increased with increasing dopant concentration in the polymers. Furthermore, the ^{1}H MAS NMR linewidths of DopedPAN (*x* $HClO_4$) showed little dependence on MAS speeds. In addition, similar linewidths were recorded in DopedPAN-*d*, which was prepared with aniline-*d*5 ($C_6D_5NH_2$). Based on these results, the origin of ^{1}H MAS NMR linewidths can be explained by the distribution of various arrangements of chains and/or dopants over the samples. In addition, narrow NMR linewidths suggest that the benzene rings in the polymers can undergo fast motions in the solids. Our NMR and XRD spectra suggest that the multivalent dopants H_2SO_4 and H_3PO_4 constructed polymer blocks in the solids. These blocks contribute to the low electrical conductivities of these polyaniline samples.

COMPETING INTERESTS

Authors have declared that no competing interests exist.

REFERENCES

1. Shirakawa H, Loutuis EJ, MacDiarmid AG, Chiang CK, Heeger AJ. Synthesis of electrically conducting organic polymers: Halogen derivatives of polyacetylene. (CH)x. J.C.S. Chem. Comm. 1977;578-80.
2. Chiang JC, MacDiarmid AG. Polyaniline: Protonic acid doping of the emeraldine form to the metallic regime. Synth. Met. 1986;13:193-205.
3. Genies E, Tsintavis C. Redox mechanism and electrochemical behaviour or polyaniline deposits. J. Electroanal. Chem. 1985;195(1):109-128.
4. Huang WS, Humphrey BD, MacDiarmid AG. Polyaniline, a novel conducting polymer. Morphology and chemistry of its oxidation and reduction in aqueous electrolytes. J. Chem. Soc. Faraday Trans. 1. 1986;82(8):2385-400.
5. Focke WW, Wnek GE, Wei Y. Influence of oxidation state, pH, and counterion on the conductivity of polyaniline. J. Phys. Chem. 1987;91(22):5813-8.
6. Stilwell DE, Park SM. Electrochemistry of conductive polymers: II. Electrochemical studies on growth properties of polyaniline. J. Electrochem. Soc. 1988;135(9):2254-62.
7. MacDiarmid AG, Chiang JC, Halpern M, Huang WS, Mu SL, Somasiri NLD, Wu WQ, Yaniger SI. Polyaniline: Interconversion of metallic and insulating forms. Mol. Cryst. Liq. Cryst. 1985;121: 173-180.
8. Maeda S. Corrosion protection of metals by conductive polymer polyaniline. J. Jpn. Soc. Colour Mater. 2012;85:240–248.
9. MacDiarmid AG, Chiang JC, Richter AF, Epstein AJ. Polyaniline: A new concept in conducting polymers. Synth. Met. 1987;18: 285-90.
10. MacDiarmid AG, Epstein AJ. Polyanilines: A novel class of conducting polymers. Faraday Discuss. Chem. Soc. 1989;88: 317-32.
11. Epstein AJ, MacDiarmid AG. Structure, order and the metallic state in polyaniline and its derivatives. Synth. Met. 1991;41: 601-6.
12. Pouget JP, Laridjani M, Jozefowicz ME, Epstein AJ, Scherr EM, MacDiarmid AG. Structural aspects of the polyaniline family of electronic polymers. Synth. Met. 1992; 51:95-101.
13. MacDiarmid AG. Polyaniline and polypyrrole: Where are we headed? Synth. Met. 1997;84:27-34.
14. Prigodin VN, Epstein AJ. Nature of insulator–metal transition and novel mechanism of charge transport in the metallic state of highly doped electronic polymers. Synth. Met. 2002;125:43-53.
15. Peo M, Forster H, Menke K, Gardner JA, Roth S, Dransfeld K. Absence of knight-shift in the metallic state of polyacetylene. Solid State Commun. 1981;38(6):467-8.
16. Hjertberg T, Salaneck WR, Lundstrom I, Somasiri NLD, MacDiarmid AG. A 13C CP-MAS NMR investigation of polyaniline. J. Polym. Sci., Polym. Lett. 1985;23(10): 503-8.
17. Kaplan S, Conwell EM, Richter AF, MacDiarmid AG. Solid-state carbon-13 NMR characterization of polyanilines. J. Am. Chem. Soc. 1988;110:7647-51.

18. Stein PC, Hartzell CJ, Jorgensen BS, Earl WL. CP-MAS studies of polyaniline. Synth. Met. 1989;29:297-302.
19. Kaplan S, Conwell EM, Richter AF, MacDiarmid AG. A solid-state NMR investigation of the structure and dynamics of polyanilines. Synth. Met. 1989;29:235-42.
20. Richter AF, Ray A, Ramanathan KV, Manohar SK, Furst GT, Opella SJ, MacDiarmid AG. ^{15}N NMR of polyaniline. Synth. Met. 1989;29:243-9.
21. Kolbert AC, Caldarelli S, Thier KF, Sariciftci NS, Cao Y, Heeger AJ. NMR evidence for the metallic nature of highly conducting polyaniline. Phys. Rev. B. 1995;51:1541-5.
22. Espe MP, Mattes BR, Schaefer J. Packing in amorphous regions of hydrofluoric-acid-doped polyaniline powder by ^{15}N–^{19}F REDOR NMR. Macromolecules. 1997; 30(20):6307-12.
23. Kababya S, Appel M, Haba Y, Titelman GI, Schmidt A. Mechanism of phenolic polymer dissolution: Importance of acid−base equilibria. Macromolecules. 1999;32(16):5337-43.
24. Sahoo SK, Nagarajan R, Roy S, Samuelson LA, Kumar J, Cholli AL. An enzymatically synthesized polyaniline: A solid-state NMR study. Macromolecules. 2004;37(11):4130-4138.
25. Blann WG, Fyfe CA, Lyerla JR, Yannoni CS. High-resolution carbon-13 NMR study of solid .pi.-.pi. molecular complexes using "magic angle" spinning techniques. J. Am. Chem. Soc. 1981;103(14):4030-3.
26. Terao T, Meada S, Yamaga T, Akagi K, Shirakawa H. ^{13}C high-resolution NMR study of doped polyacetylene. Solid State Commun. 1984;49(8):829-32.
27. Osterholm JE, Sunila P, Hjertberg T. ^{13}C CP-MAS NMR and FTIR studies of polythiophenes. Synth. Met. 1987;18:169-76.
28. Grobelny J, Obrzut J, Karasz FE. Solid-state ^{13}C NMR study of neutral insulating and electrochemically doped conducting poly (p-phenylene vinylene). Synth. Met. 1989;29:97-102.
29. Wehrle B, Limbach HH, Mortensen J, Heinze J. Solid-state ^{15}N CPMAS NMR study of the structure of polypyrrole. Synth. Met. 1990;38:293-8.
30. Chaloner-Gill B, Euler WB, Mumbauer PD, Roberts JE. Direct evidence of a bipolaron charge carrier in conducting polyazines from carbon-13 and nitrogen-15 solid-state NMR spectroscopy: Detection of a nitrenium cation by natural abundance ^{15}N solid-state NMR spectroscopy. J. Am. Chem. Soc. 1991;113(18):6831-4.
31. Wehrle B, Limbach HH, Morteensen J, Heinze J. ^{15}N CPMAS NMR study of the structure of polyaniline. Angew. Chem., Int. Engl. Adv. Mater. 1989;28(12):1741-3.
32. Kenwright AM, Feast WJ, Adams P, Milton AJ, Monkman AP, Say BJ. Solution state NMR studies of polyaniline structure. Synth. Met. 1993;55:666-71.
33. Mathew R, Yang D, Mattes BR, Espe MP. Effect of elevated temperature on the reactivity and structure of polyaniline. Macromolecules. 2002;35(20):7575-81.
34. Young TL, Espe MP, Yang D, Mattes BR. Application of solid-state NMR to characterize the interaction of gel inhibitors with emeraldine base polyaniline. Macromolecules. 2002;35(14):5565-9.
35. Wang X, Sun T, Wang C, Wang C, Zhang W, Wei Y. ^{1}H NMR determination of the doping level of doped polyaniline. Macromolecular Chemistry and Physics. 2010;211:1814-9.
36. Nakano R, Honda H, Kimura T, Kyo S, Ishimaru S, Miyake R, Nakata E, Takamizawa S, Noro S. Anomalous H/D isotope effect on ^{35}Cl NQR frequencies and H/D isotope effect on ^{1}H MAS NMR spectra in pyrrolidinium *p*-Chlorobenzoate. Bull. Chem. Soc. Jpn. 2010;83(9):1019-29.
37. Honda H, Kyo S, Akaho Y, Takamizawa S, Terao H. H/D isotope effect of ^{1}H MAS NMR spectra and ^{79}Br NQR frequencies of piperidinium *p*-bromobenzoate and pyrrolidinium *p*-bromobenzoate. Hyperfine Interactions. 2011;197:275-285.
38. Nakano R, Honda H, Ishimaru S, Noro S. ^{1}H MAS, ^{13}C CP/MAS, and ^{2}H NMR spectra studies of piperidinium *p*-chlorobenzoate. Hyperfine Interactions 2013;222:43-54.
39. Honda H. ^{1}H-MAS-NMR chemical shifts in hydrogen-bonded complexes of chlorophenols (Pentachlorophenol, 2,4,6-Trichlorophenol, 2,6-Dichlorophenol, 3,5-Dichlorophenol, and *p*-Chlorophenol) and amine, and H/D isotope effects on ^{1}H-MAS-NMR spectra. Molecules 2013;18(4): 4786-4802.
40. Hayasaki T, Hirakawa S, Honda H. New ionic plastic crystals of NR_4BEt_3Me (R = Me, Et) and $NR_xR'_{4-x}BEt_3Me$ (R = Et, R' = Me, Pr, x = 1-3) in a new class of plastic

crystals. Bull. Chem. Soc. Jpn. 2013;86(8): 993-1001.

41. Morita T, Honda H, Katayama T, Tanaka S, Ishimaru S. Cation-type dependences of ^{1}H and ^{29}Si MAS NMR chemical shifts and desorption temperatures of water molecules in faujasite-type zeolites. Int. Res. J. Pure and Applied Chem. 2014;4(6): 638-55.
42. Hayasaki T, Hirakawa S, Honda H. Investigation of new ionic plastic crystals in Tetraalkylammonium Tetrabuthylborate. Z. Naturforsch. 2014;69a:433-40.
43. Hirakawa S, Honda H. ^{1}H and ^{13}C NMR and electrical conductivity studies on new ionic plastic crystals of Tetraalkylammonium Tetraethylborate. Z. Naturforsch. 2015;70a:521-8.
44. Hirakawa S, Kotani Y, Hayasaki T, Honda H. New ionic plastic crystals formed from cage-type cations consisting of 1-alkyl-4-aza-1-azoniabicyclo[2,2,2]octane with BEt_3Me, BEt_4, and BBu_4 Anions. Bull. Chem. Soc. Jpn. 2015:88(12):1735-45.
45. Masuda A, Morita T, Itayama N, Yakushi Y, Akiike M, Kawaguchi T, Honda H, Ishimaru S. Removing Diethylphthalate from water systems using zeolites and mesoporous materials. Journal of Progressive Research in Chemistry. 2016; 3(2):143-57.
46. Gerstein BC, Dybowski CR. Transient techniques in NMR of solids. Academic Press; 1985.
47. Slichter CP. Principles of magnetic resonance. 3rd. Springer; 1990.
48. Sapurina IY, Shishov MA. New polymers for special applications. Chapter 9. InTech; 2012.

Peer-review history:
The peer review history for this paper can be accessed here:
http://sciencedomain.org/review-history/17793